Heat Mass Transfer (2008) 44:857–864
DOI 10.1007/s00231-007-0302-3

ORIGINAL

Convective heat transfer in single-phase flow in a vertical tube subjected to axial low frequency oscillations

Rajashekhar Pendyala · Sreenivas Jayanti · A. R. Balakrishnan

Received: 18 October 2006 / Accepted: 8 June 2007 / Published online: 19 July 2007

Abstract The effect of oscillations on the heat transfer in a vertical tube has been studied experimentally. A vertical tube was mounted on a plate and the whole plate was subjected to oscillations in the vertical plane using a mechanical oscillator to provide low frequency oscillations. A section of the tube in the middle is subjected to a constant heat flux. The effect of the oscillations on the heat transfer coefficient has been examined. It was found that the heat transfer coefficient increased with oscillations in the laminar regime. In turbulent flow regime ($Re > 2{,}100$) it is found that the effect of oscillations did not show any change. A correlation has been developed for enhancement of the local Nusselt number in terms of the effective acceleration and Reynolds number. Using this, an expression has been proposed to calculate the mean Nusselt number as a function of the tube length.

List of symbols

a	acceleration (m/s^2)
D	diameter of pipe (m)
g	gravitational acceleration (m/s^2)
Gz	Graetz number
h_x	local heat transfer coefficient (W/m^2 °C)
k	thermal conductivity (W/m °C)
L	length of the tube (m)
$Nu_{m,os}$	mean Nusselt number under oscillating conditions
$Nu_{m,s}$	mean Nusselt number at steady state
Nu_x	local Nusselt number
$Nu_{x,os}$	local Nusselt number under oscillating conditions
$Nu_{x,s}$	local Nusselt number at steady state
Pr	Prandtl number
q	heat flux (W/m^2)
Re	Reynolds number
T_{bx}	bulk liquid temperature (°C)
T_{wx}	tube wall temperature (°C)
Q	volumetric flow rate (m^3/s)
$\overline{\Delta Q}$	magnitude of variation in flow rate (m^3/s)
x	axial distance (m)
ω	frequency (radians/s)

R. Pendyala · S. Jayanti · A. R. Balakrishnan (✉)
Department of Chemical Engineering,
Indian Institute of Technology Madras,
Chennai 600036, Tamil Nadu, India
e-mail: arbala@iitm.ac.in

1 Introduction

Barge-mounted floating nuclear plants offer an attractive alternative to land-based power plants to drive desalination plants to provide drinking water for coastal communities. Some of the advantages of barge-mounted nuclear reactors are lower land cost and lesser construction time, simpler anti-seismic design measures and decommissioning technology [1, 2]. The main difference from a heat transfer point of view between land-based and barge-mounted equipment is the influence of sea wave oscillations on the latter. The thermal hydraulic behaviour of barge-mounted equipment is influenced by different motions such as heaving, rolling and pitching [3] that the barge is subjected to. Oscillations change the effective forces acting on the fluid (gravitational, pressure and frictional) and induces flow fluctuations [4, 5], which result in a change in momentum, heat and mass transfer characteristics. In some

cases, the change is beneficial, for example, in the form of increased heat and mass transfer rates. However, the fluctuations in the flow rate and pressure drop may induce further flow instabilities in equipment involving phase change and may have a deleterious effect on their performance. For example, studies [6, 7] indicate that the critical heat flux in a steam generating tube may be reduced by as much as 50% in case of severe oscillations. The objective of the present study is to examine the effect of such oscillations on the single-phase heat transfer characteristic.

Oscillating and pulsating flows have been studied both experimentally and theoretically for a number of decades. In one of the earliest experimental studies, Martinelli et al. [8] obtained an increase of 10% in the Nusselt number for the Reynolds number range 300–2,000 and frequency range 13–265 cycles/min. Similar increase of the heat transfer coefficient under pulsating flow conditions has been reported by a number of investigators [9–12]. Enhanced mass transfer rates in a pulsed column have been achieved [13] by inducing pulsations either by liquid pulsing or by using reciprocating sieve plates in the column. This augmentation of heat and mass transport was attributed to changes in the lateral diffusion, accumulation near the wall and convective motion forced by the oscillation. Pulsations can also reduce the thickness of the thermal/concentration boundary layer near the wall and therefore decreases the thermal/mass transfer resistance [9].

Analytical and numerical studies of flow and heat transfer in pulsating flow in a circular tube have been reported in the recent literature. An analytical expression for the oscillating velocity profile in fully developed laminar flow subjected to a periodically varying pressure gradient is given by Schlichting [4]. The corresponding case of flow with wall oscillations has been studied experimentally and theoretically by Clamen and Minton [5]. While good agreement was found between theory and experiment at low Reynolds numbers, considerable deviation was found at higher Reynolds numbers. The experimental data seemed to indicate the flow rate fluctuations to be less intense than predicted. Direct measurement of the induced flow rate fluctuations by the present authors [14] showed that the intensity of flow rate fluctuations decreased with increasing Reynolds number. Numerical studies of heat transfer under imposed flow oscillations have been conducted by a number of researchers [15–24].

The results of Cho and Hyun [15] and Kim et al. [16] showed that the heat transfer rate may either increase or decrease and that the effect of pulsation was more pronounced at higher amplitudes of pulsation, lower Prandtl numbers and in the entrance region. The effect on Nusselt number was more noticeable at low and moderate frequencies; while at higher frequencies the heat transfer was found to be unaffected. Similar results were also obtained by Moschandreou and Zamir [17], Guo and Sung [18] and Yu et al. [19].

In addition to these theoretical studies, a number of experimental studies of heat transfer in pulsating flow conditions have been reported. Gbadibo et al. [20] found enhancement and reduction in the heat transfer coefficient in their experimental study of the thermal entrance region in a pipe using air in the turbulent flow region with uniform heat flux. The improvement in mean Nusselt number peaked at a particular pulsating frequency depending on the Reynolds number. Similar results were also reported by Habib et al. [21] and Zohir et al. [22]. Baird et al. [12], Mamayev et al. [23] and Liao and Wang [24] conducted heat transfer experiments under pulsating turbulent flow conditions. They found that pulsations improve the heat transfer in the turbulent flow only at sufficiently high amplitudes to cause flow reversal for part of the cycle.

Thus, there is a vast amount of literature on experimental and theoretical studies of the effect of pulsation on the heat transfer in pipe flow. While a broad range of flow conditions, namely, Reynolds number, frequency and amplitude of pulsation, have been covered, all the available results have been obtained under liquid pulsing conditions. Most of the results obtained have also been for cases in which the effective acceleration due to oscillations is rather large (either due to large frequency or large pulsation amplitude) compared to that encountered in typical sea-wave induced oscillations where oscillations have a maximum frequency of about 0.5 Hz and a maximum effective acceleration of 0.1 g [6]. The objective of the present work is to investigate the effect of pipe oscillations on the convective heat transfer for pulsations induced by *wall oscillations*. To this end, single-phase heat transfer experiments have been conducted in an oscillating tube in which the instantaneous wall temperature and the fluid temperature have been measured in a tube with an imposed, uniform heat flux. The parameters studied include the effective acceleration (a/g) and the Reynolds number. Details of the experiments and the results obtained are discussed below.

2 Experimental set-up

2.1 The flow loop

The schematic diagram of the experimental set up is shown in Fig. 1. The test section consists of a vertical stainless steel tube of 16 mm ID, wall thickness of 2 mm and a length of 1.75 m. The ends of the tube were connected to the rest of the test loop by flexible hoses. A central section of length 0.55 m of the tube, electrically insulated from the rest using Teflon washers and was heated electrically using DC power supply from a 28.8 kVA rectifier with copper

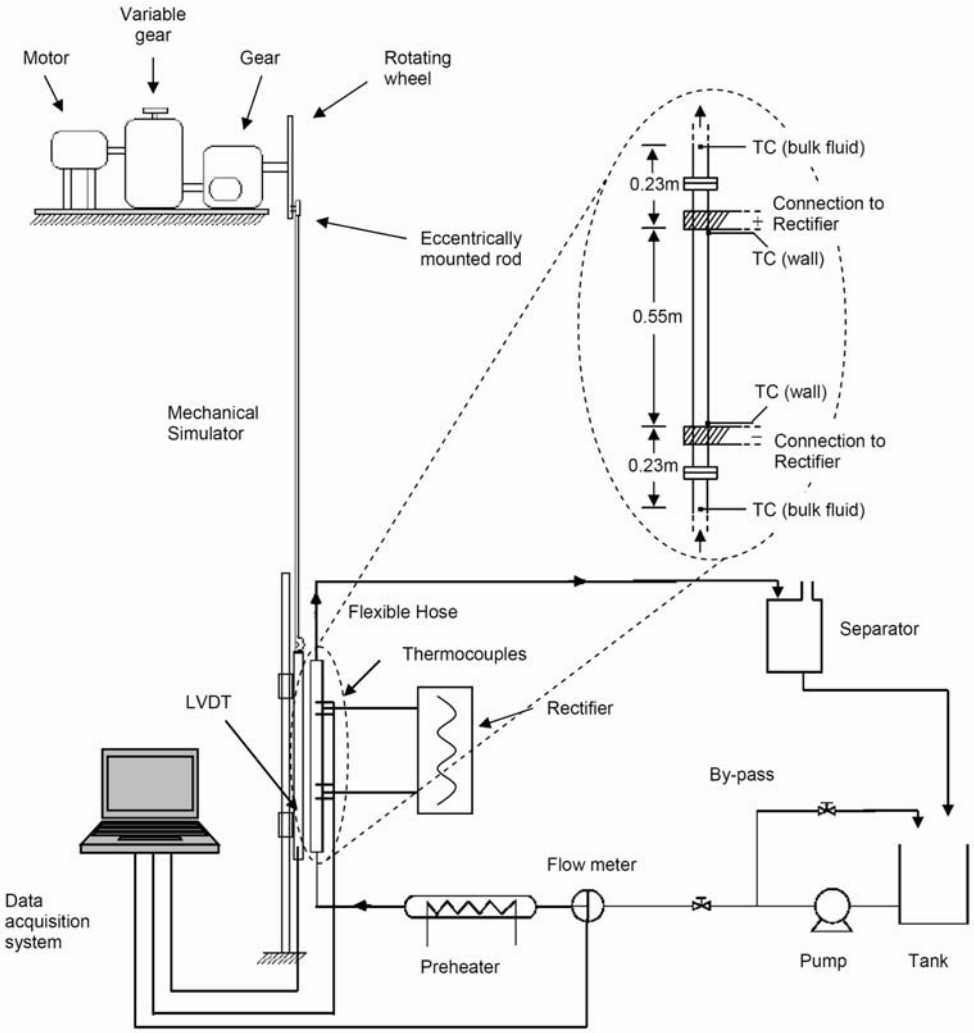

Fig. 1 Schematic diagram of the test loop

cables clamped at both ends. Thus, the heated section of the pipe is 34 diameters long and is connected at either end by calming sections of 38 diameters length. The test section is insulated with asbestos rope of 3-mm thick, wound three layers over the heated length. The electrical connection to the rectifier is by copper cables which are flexible, to enable the test section to oscillate. Power input to the test section was varied using a step-up/step-down arrangement in the rectifier. A 1.12 kW (1.5 hp) multistage centrifugal pump was used to pump water from a storage tank to the test section. A by-pass valve is provided to recycle excess liquid, which is pumped back to the storage tank. A needle valve is used to control the flow to the test section and a gate valve is used to control the bypass. A pre-heater was used to control the temperature of the water at tube inlet. The pre-heater is a stainless steel cylindrical vessel with 5 kW immersion heater. An on/off controller regulates the outlet temperature of the pre-heater, so that the inlet temperature to the test section can be maintained at the desired level. The heated fluid from the test section is discharged into an open tank (which may serve as a steam separator in case steam is produced) and is drained eventually to the water tank connected to the pump. Thus, there is no direct feedback of the flow rate oscillations in the test section to the pump intake. While the water tank temperature slowly rises over the course of the experiment, the temperature at the inlet to the test section is kept constant using the pre-heater. Thus, it can be stated that there is no coupling between the test section outlet and inlet.

2.2 Mechanical oscillator

A mechanical oscillator, consisting of an eccentrically mounted connecting rod device [14], was used to generate the low frequency oscillations in the test section. It consists of a three-phase motor rotating a constant speed of 1,440 rpm, a mechanical gear box to reduce the shaft speed to the desired range of 8–30 rpm, and a connecting rod mounted eccentrically on a disk attached to the shaft. The eccentric rod arrangement converts the rotational motion of

the motor shaft to a vertical, oscillatory motion of the connecting rod.

The test section was fixed on to a plate, which is attached to the connecting rod. Well-lubricated guide shafts were provided at the ground level to keep the motion of the plate smooth and vibration free. To maintain structural integrity, the test section was connected to the rest of the flow loop with flexible hose connections. The mechanical oscillator can produce heaving motion with an amplitude of 0.125 m with a period of oscillation varying from 8 to 30 cycles/min, which is equivalent to an acceleration in the range of 0.1–1.125 m/s^2. A variable reduction gear was used to set the test section oscillation period manually at the desired value.

2.3 Instrumentation

The wall and the fluid temperatures were measured using Chromel–Alumel thermocouples (K-type). The thermocouples are silver-brazed into grooves of depth 1 mm on the test section. The bulk fluid temperature was measured at the inlet to the test section and at an axial distance of 0.23 m from the end of the heated section at the outlet. Wall temperatures were measured at an axial distance of 1 mm from the end of the heated section at the outlet. The power input to the test section is estimated from the product of the voltmeter and ammeter readings. The voltage drop across the test section was measured using a voltmeter connected to two ends of the test section and the current was recorded from an ammeter located in the rectifier. A linear variable displacement transducer (LVDT) was used to track the displacement of test section with time from which the frequency and the time period of oscillations were obtained. An orifice flow meter fixed after the outlet of the pump was used to measure the flow rate. The orifice meter is connected to a differential pressure transducer, which measures the pressure difference online. Calculations show that the flow rate measuring system has adequate dynamic response.

A computer-based data acquisition system with analogue-to-digital (A/D) cards was used to record the instantaneous position (displacement) of the test section, the flow rate, the pressure drop in the test section and the temperatures. The voltages from thermocouples were amplified to the required range needed for the data acquisition system. A data-sampling rate of 250 samples per second has been found to offer sufficient resolution of the transients in the frequency ranges of interest.

3 Experimental procedure

Experiments were conducted over a range of oscillation frequencies and flow rates. Oscillation periods were varied from 2 to 8 s for different flow rates covering the Reynolds number range of 500–6,500. The measured LVDT reading was used to determine the kinematics of the tube oscillations. The wall heat flux was varied in the range of 3.4–10.8 kW/m^2. The temperatures were measured for a period of 300 s for each flow condition after reaching steady state. The local heat transfer coefficient at the end of heated length was obtained from the imposed wall heat flux and the measured values of the wall and the bulk fluid temperature by

$$h_x = \frac{q}{(T_{wx} - T_{bx})} \tag{1}$$

where h_x is the local heat transfer coefficient, q is the wall heat flux, T_{wx} and T_{bx} are the wall and the bulk temperatures at the end of the heated section. The local Nusselt number is then given by

$$Nu_x = \frac{h_x D}{k} \tag{2}$$

where k is the water thermal conductivity evaluated at the bulk temperature of water.

The rig was commissioned by conducting experiments under non-oscillating conditions. The heat transfer coefficients found under laminar and turbulent flow conditions agreed well with well-established empirical correlations as shown in Fig. 2, where the measured Nusselt number is compared with that obtained from the Graetz analysis for laminar flow conditions [25] and that obtained from the correlation of Hausen [26] for turbulent flow conditions.

3.1 Data reduction

The data reduction was achieved from the measurement of four primary parameters, namely, the displacement from which the frequency, amplitude and thus the effective

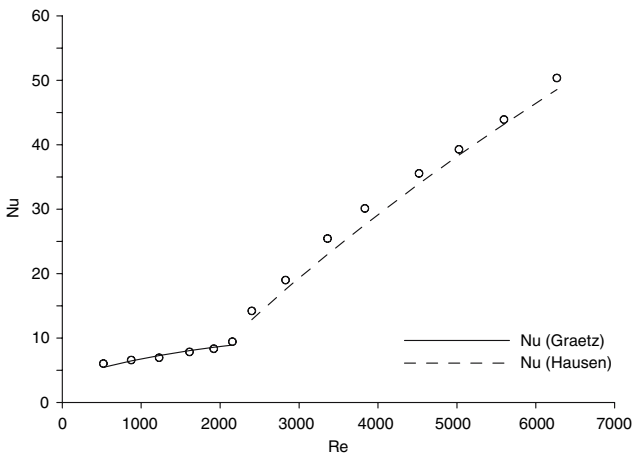

Fig. 2 Heat transfer without oscillations

gravity have been obtained; the pressure drop across the orifice flow meter to measure the flow rate; the voltage and the current measurements from which the imposed wall heat flux is determined; and the wall and the bulk fluid temperatures at inlet and outlet using which the heat transfer coefficient is calculated. The resolution of the data acquisition system used in the present study is 10^{-4} V out of a maximum of 10 V. Using the calibration curves, this corresponds to a resolution in the measurement of pressure at ±0.25 N/m^2, in the LVDT displacement at ±0.015 mm, in temperature at ±0.1°C. The resolution of voltmeter and the ammeter used in the DC heating of the tube are 0.001 V and 10 A, respectively.

The highest frequency of the imposed oscillations in the experiments is 30 cycles/min. It is possible for higher frequency oscillations (vibrations) to appear if the motion of the mechanical oscillator is not smooth. In order to resolve these and any flow-related higher harmonics, which may appear in the measured variables, data sampling is carried out at a sampling rate of 250 Hz, which would allow frequencies of 125 Hz to be resolved without aliasing errors. The data analysis has been done using MATLAB. The digital data are smoothened using the Savitzky–Golay filter, which is a digital polynomial filter. The flow rate is obtained based on the instantaneous pressure difference obtained from the filtered pressure transducer signal. The wall heat flux is practically unaffected by the tube oscillation and is obtained from the manual reading of the voltmeter and the ammeter. Since the thermal capacity of the heated tube has an unquantified role in the transient temperature distribution and since the temperature oscillations are in any case very small, the heat transfer coefficient is obtained from a cycle-averaged reading of the thermocouples.

4 Results and discussion

Heat transfer measurements have been carried out over a range of flow rates, heat fluxes and frequencies of oscillation. The effect of acceleration on the wall and the bulk temperatures at the end of the heated section is shown in Fig. 3. Here, the wall and the bulk fluid temperatures recorded by the data acquisition system over a short period of 4 s, is shown for different frequencies of oscillation at a fixed Reynolds number of 1,000 and a heat flux of 10.66 kW/m^2. Typically, the temperature traces did not exhibit significant oscillations corresponding to the forcing frequency, presumably due to conduction effects within the wall and within the fluid. It is seen from Fig. 3 that as the frequency of oscillation increases, the outlet bulk temperature remains more or less constant while the wall temperature at the end of the heated section decreases. This

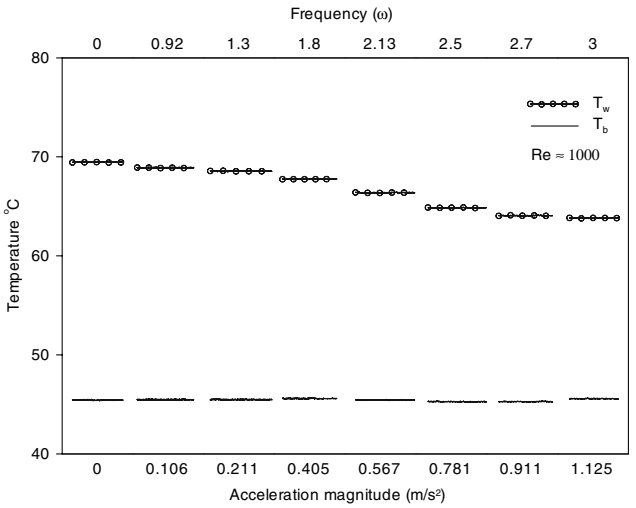

Fig. 3 Wall and the bulk temperatures recorded by the data acquisition system for different oscillation acceleration magnitudes at a fixed Reynolds number of about 1,000

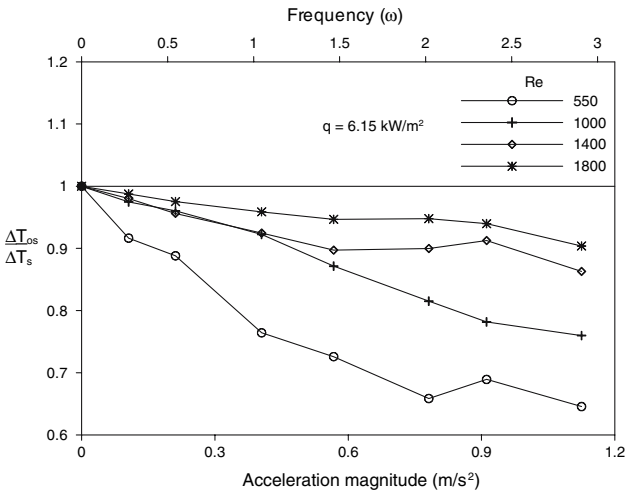

Fig. 4 Ratio of wall-to-bulk temperature differences for different oscillation acceleration magnitudes at different Reynolds numbers at a heat flux of 6.15 kW/m^2

shows that that the heat transfer coefficient under oscillating conditions increases as the oscillation frequency increases.

The effect of Reynolds number on temperature driving force and therefore the heat transfer coefficient under oscillating and non-oscillating conditions is shown in Fig. 4. That is the ratio of the wall-to-bulk temperature difference under oscillating conditions to that under non-oscillating conditions at different Reynolds numbers and at different frequencies of oscillation. Typically, this ratio of temperature difference is found to be decreasing as the frequency increases, which confirms the trend shown in Fig. 3 that increased acceleration increases heat transfer enhancement. The relative enhancement appears to be

significantly higher at low Reynolds numbers, which is in agreement with earlier results in liquid pulsing experiments discussed earlier. Measurements of the induced flow rate fluctuations by the imposed tube oscillations showed that the relative magnitude of flow rate fluctuation, i.e. magnitude of the fluctuating flow rate (rms) divided by the mean flow rate, is related to the Reynolds number as

$$\frac{\overline{\Delta Q}}{\overline{Q}} = 83000 \cdot \left(\frac{a}{g}\right) \frac{1}{Re^{1.5}} \tag{3}$$

In the present case the relative amplitude of flow rate fluctuation varied between 0.74 at a *Re* of 550–0.125 at a *Re* of 1,800. Thus, the relatively large enhancement of the heat transfer coefficient at low *Re* appears to be related to the relatively large amplitudes of flow rate fluctuations. In this sense, the present results are consistent with those for the liquid pulsing case.

4.1 Heat transfer under laminar flow conditions

The Nusselt number at the end of the heated section (*L/D* = 34.3) has been calculated from the measurements of the local wall and bulk temperatures. The variation of this local Nusselt number with Reynolds number and the effective acceleration is shown in Fig. 5 for laminar flow conditions (assuming the transition to turbulence is unaffected by the low frequency oscillations). Also shown here for reference is the measured variation under steady, non-oscillating conditions. This also corresponds to the classical Graetz solution for laminar flow in the entrance region. It can be seen that there is an increase in local Nusselt number under pulsating conditions compared to that obtained under steady flow values. As noted before, the enhancement is higher at higher effective accelerations and lower Reynolds numbers. The highest improvement is found at low Reynolds numbers and high magnitude of oscillation acceleration. The Nusselt number is increased by about 60.3% compared to steady flow at Reynolds number 567 and a magnitude of oscillation acceleration of 1.125 m/s^2.

The local Nusselt number is affected not only by the pulsations but also by entrance length effects. Graetz analysis for the Nusselt number in the thermal entrance region [27] shows that the local Nusselt number under steady flow ($Nu_{x,s}$) is given by where Gz is the dimensionless Graetz number and is given by

$$\begin{aligned} Nu_{x,s} &= 1.302 \cdot Gz^{1/3} - 1 && \text{for } (1/Gz) \le 0.00005 \\ &= 1.302 \cdot Gz^{1/3} - 0.5 && \text{for } 0.00005 \le (1/Gz) \le 0.0015 \\ &= 4.364 + 8.68(10^3/Gz)^{-0.506} e^{-14/Gz} && \text{for } (1/Gz) \ge 0.0015 \end{aligned} \tag{4}$$

$$Gz = \frac{Re \cdot Pr}{x/D} \tag{5}$$

A correlation for the local Nusselt number under oscillating conditions ($Nu_{x,os}$) can now be sought in the form

$$Nu_{x,os} = f(x/D,\ Re,\ Pr,\ a/g,\ Nu_{x,s}) \tag{6}$$

Using the present data, the following correlation is proposed for the enhancement of local Nusselt number due to oscillations:

$$\frac{Nu_{x,os}}{Nu_{x,s}} = 1 + 150 \cdot \frac{x/D}{Re \cdot Pr} \cdot \left(\frac{a}{g}\right)^{0.75} \tag{7}$$

The performance of the correlation is shown in Fig. 6 (parity plot); the agreement is within ±11.4%.

The mean Nusselt numbers can be calculated by integration of the local Nusselt number over the entire heated length. The mean Nusselt number can be computed from

$$Nu_{m,os} = \frac{1}{L}\int_0^L Nu_{x,os}dx \tag{8}$$

$$= \frac{1}{L}\int_0^L Nu_{x,s}dx + 150 \cdot \frac{1}{L}\int_0^L \frac{Nu_{x,s}}{Gz}\left(\frac{a}{g}\right)^{0.75} dx \tag{9}$$

$$= Re \cdot Pr \frac{D}{L}\left\{ \int_0^{Gz_L^{-1}} Nu_{x,s} d(Gz^{-1}) + 150 \cdot \int_0^{Gz_L^{-1}} \frac{Nu_{x,s}}{Gz}\left(\frac{a}{g}\right)^{0.75} d(Gz^{-1}) \right\} \tag{10}$$

Here, $Nu_{x,s}$ is given by Eq. (4) which can also be used to obtain the mean Nusselt number under steady, non-oscillating flow conditions for a specified *Re* and *L/D*.

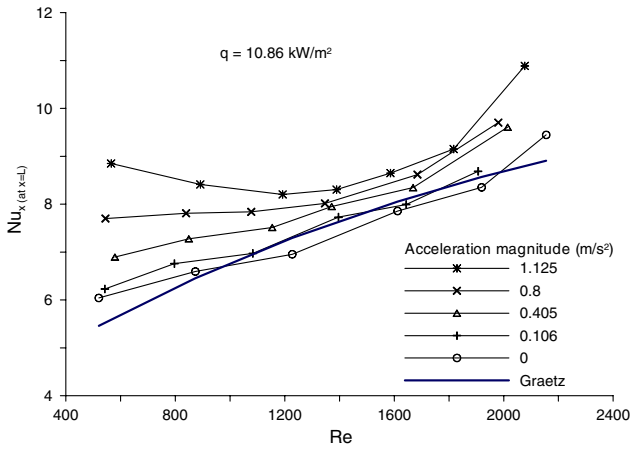

Fig. 5 Nusselt number at different Reynolds numbers at different acceleration magnitudes in laminar flow conditions at a heat flux of 10.86 kW/m^2

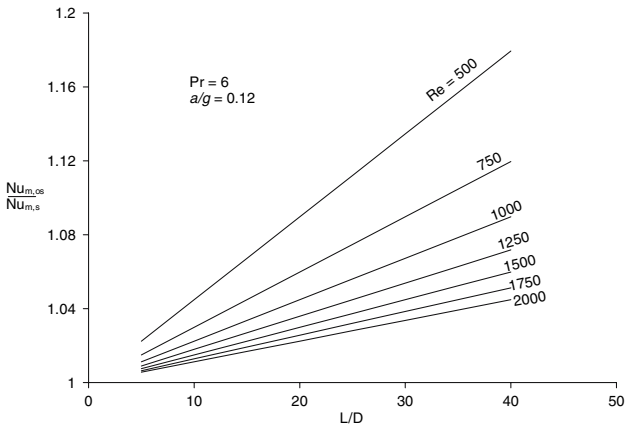

Fig. 7 Ratio of Nusselt number under oscillations and under steady conditions for different *L/D* and Reynolds number at *Pr* = 6 and *a/g* = 0.12

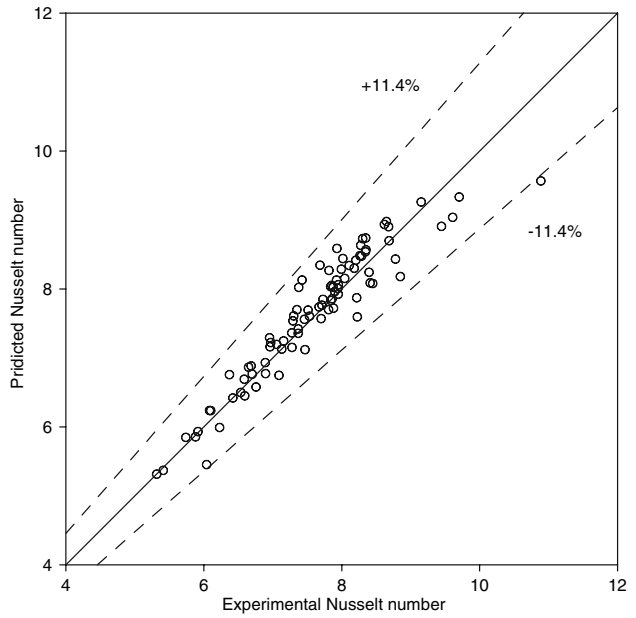

Fig. 6 Performance of the correlation for predicting the enhancement of local Nusselt number under laminar flow conditions

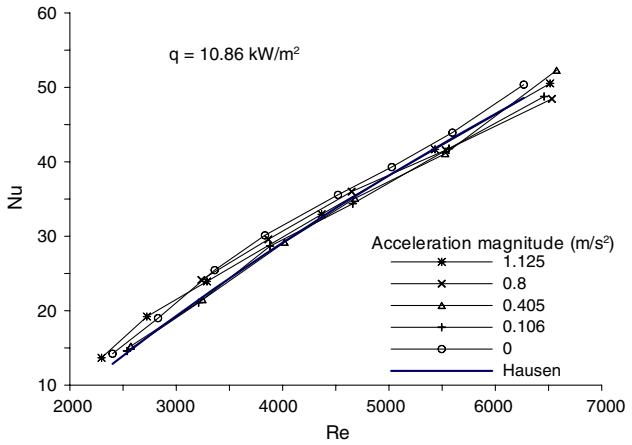

Fig. 8 Nusselt number against Reynolds number for different acceleration magnitudes in turbulent flow conditions at a heat flux of 10.86 kW/m^2

Typical variation of ($Nu_{m,os}/Nu_{m,s}$) for different *L/D* and Reynolds numbers is shown in Fig. 7 for a Prandtl number of 6. It can be seen that as *L/D* increases, the enhancement of the mean Nusselt number is higher. It is found that this parametric dependence on *L/D*, Re and *a/g* can be expressed by the following simple correlation

$$\frac{Nu_{m,os}}{Nu_{m,s}} = 1 + 62.5 \cdot \frac{L/D}{Re \cdot \mathrm{Pr}} \cdot \left(\frac{a}{g}\right)^{0.75} \tag{11}$$

The correlation agrees within ±1.5% error on numerical integration (Eq. 9) and can be used to determine the net enhancement of mean Nusselt number by the oscillations.

4.2 Heat transfer in turbulent regime

There is not much change in the heat transfer rate in the turbulent regime. The dependence of the Nusselt number on Reynolds numbers at varying magnitudes of oscillation acceleration in the turbulent regime at a heat flux of 10.86 kW/m^2 is shown in Fig. 8. This may be due to the magnitude of flow fluctuations being very low.

4.3 Uncertainty analysis

The relative uncertainty in the deduced parameters such as the heat flux and the Nusselt number has been estimated using the method due to Moffat [28]. In the present study the measured variables are displacement, flow rate and temperatures. The uncertainty in measurement of voltage and current is 1 and 1.5%. Therefore, the uncertainty in

estimating heat flux is ±1.8%. The uncertainty in the measurement of temperature is ±1%. As a result, the uncertainty in Nusselt number is ±2.06%. The uncertainty in the measurement of displacement is ±0.1%. Therefore, the uncertainty in estimating effective acceleration is ±0.22%. The measurement uncertainty in flow rate is ±2%. Therefore the relative uncertainty in the enhancement in Nusselt number is estimated to be ±2.1%.

5 Conclusions

The results obtained from the experiments show that the influence of an externally imposed periodic oscillation on the heat transfer is stronger at lower flow rates. In laminar flow conditions, the oscillations improved the heat transfer coefficient. The highest improvement is found at low Reynolds numbers and high magnitude of oscillation acceleration. The empirical dimensionless equations for enhancement in local and mean heat transfer rates have been proposed. This is applicable in the laminar regime for a Reynolds number range of $500 < Re < 2{,}100$ and dimensionless effective acceleration range of $0 < a/g < 0.115$. However, the effect is negligible at higher flow rates i.e. in the turbulent regime.

References

1. Humphries JR, Davies K (1998) A floating desalination/co-generation system using the KLT–40 reactor and Canadian RO desalination technology. In: Proceedings of advisory group meeting, vol 1172. International Atomic Energy Agency, Vienna, IAEA-TECDOC, pp 41–52
2. Panov YK, Polunichev VI, Zverev KV (1998) Nuclear floating power desalination complexes. In: Proceedings of four technical meeting, vol 1056. International Atomic Energy Agency, Vienna, IAEA-TECDOC, pp 93–104
3. Ishida I, Kusunoki T, Murata H, Yokomura Y, Kobayashi M, Nariai H (1990) Thermal hydraulic behavior of a marine reactor during oscillations. Nucl Eng Des 120:213–225
4. Schlichting H (1979) Boundary layer theory, 7th edn. McGraw-Hill, New York
5. Claman M, Minton P (1977) An experimental investigation of flow in an oscillating pipe. J Fluid Mech 81:421–431
6. Isshiki N (1966) Effects of heaving and listing upon thermal hydraulic performance and critical heat flux of water cooled marine reactors. Nucl Eng Des 4:138–162
7. Otsuji T, Kurosowa A (1982) Critical heat flux of forced convection boiling in an oscillating acceleration field—I. General trends. Nucl Eng Des 71:15–26
8. Martinelli RC, Boelter LMK, Weinberg EB, Yakahi S (1943) Heat transfer to a fluid flowing periodically at low frequencies in a vertical tube. Trans ASME 65:789–798
9. Havemann HA, Rao NN (1954) Heat transfer in pulsating flow. Nature 7:41
10. West FB, Taylor AT (1952) The effect of pulsation on heat transfer in turbulent flow of water inside tubes. Chem Eng Prog 48:39–43
11. Lemlich R (1961) Vibration and pulsation boost heat transfer. Chem Eng 68:171–176
12. Baird MHI, Duncan GJ, Smith JI, Taylor J (1966) Heat transfer in pulsed turbulent flow. Chem Eng Sci 21:197–199
13. Krasuk JH, Smith JM (1963) Mass transfer in a pulsed column. Chem Eng Sci 18:591–598
14. Pendyala R, Jayanti S, Balakrishnan AR (2007) Flow and pressure drop fluctuations in a vertical tube subject to low frequency oscillations. Nucl Eng Des (in press)
15. Cho HW, Hyun JM (1990) Numerical solutions of pulsating flow and heat transfer characteristics in a pipe. Int J Heat Fluid Flow 11:321–330
16. Kim SY, Kang BH, Hyun JM (1993) Heat transfer in the thermally developing region of a pulsating channel flow. Int J Heat Mass Transfer 36:4257–4266
17. Moschandreou T, Zamir M (1997) Heat transfer in a tube with pulsating flow and a constant heat flux. Int J Heat Mass Transfer 40:2461–2466
18. Guo Z, Sung HJ (1997) Analysis of the Nusselt number in pulsating pipe flow. Int J Heat Mass Transfer 40:2486–2489
19. Yu JC, Li ZX, Zhao TS (2004) An analytical study of laminar heat convection in a circular pipe with constant heat flux. Int J Heat Mass Transfer 47:5297–5301
20. Gbadibo SA, Said SAM, Habib MA (1999) Average Nusselt number correlation in the thermal entrance region of steady and pulsating turbulent pipe flows. Heat Mass Transfer 35:337–381
21. Habib MA, Attya AM, Eid AI, Aly AZ (2002) Convective heat transfer characteristics of laminar pulsating pipe air flow. Heat Mass Transfer 38:221–232
22. Zohir AE, Habib MA, Attya AM, Eid AI (2006) An experimental investigation of heat transfer to pulsating pipe airflow with different amplitudes. Heat Mass Transfer 42:625–635
23. Mamayev VV, Nosov VS, Syromyatnikov NL (1976) Investigation of heat transfer in pulsed flow of air in pipes. Heat Transfer-Soviet Res 8:111–116
24. Liao NS, Wang CC (1988) On convective heat transfer in pulsating turbulent pipe flow. Exp Heat Transfer Fluid Mech Thermodyn, pp 536–542
25. Ozisik MN (1985) Heat transfer a basic approach. McGraw-Hill, New York
26. Hausen H (1983) Heat transfer in counterflow, parallel-flow, and cross-flow. McGraw-Hill, New York
27. Shah RK, Bhatti MS (1987) Laminar convective heat transfer in ducts. In: Kakac S, Shah RK, Aung W (eds) Hand book of single-phase convective heat transfer, Wiley, New York
28. Moffat RJ (1988) Describing the uncertainties in experimental results. Exp Therm Fluid Sci 1:3–17